




Cite this: *Toxicol. Res.*, 2018, 7, 258

## Bixin protects against particle-induced long-term lung injury in an NRF2-dependent manner†

Lian Xue,<sup>‡</sup> Hong Zhang,<sup>‡</sup> Jie Zhang,<sup>b</sup> Bingyan Li,<sup>c</sup> Zengli Zhang<sup>\*b</sup> and Shasha Tao <sup>\*a,b</sup>

**Scope:** Particle-induced lung injury is a kind of comprehensive pulmonary disease with not only inflammation but also fibrosis. Bixin is a natural compound that is widely used as a food additive. Our previous studies demonstrated that bixin could alleviate inflammation in ventilation-induced acute lung injury as well as UV-exposure caused skin damage. But whether it could depress silica-induced long-term comprehensive lung injury and the mechanism of bixin in this protection have not yet been studied. **Methods:** A murine SiO<sub>2</sub>-induced long-term comprehensive lung injury model was established through silica intra-tracheal instillation. To elucidate the effects and mechanisms of bixin in silica-induced pulmonary inflammation and fibrosis, we treated mice with bixin following silica instillation. **Results:** Bixin treatment attenuated the accumulation of inflammatory cells which significantly ameliorated pathological inflammation and fibrotic development in the lungs. In addition, intraperitoneal (i.p.) injection of bixin in mice led to the upregulation of the NRF2 response in the lungs. Since alveolar macrophage activation plays a vital role in the initiation and progression of this injury, the mechanism was further studied in the THP-1 macrophage cells. Bixin activated NRF2 signals via blocking KEAP1 mediated ubiquitylation and degradation of NRF2. **Conclusions:** Our work has brought insights into exploring anti-particle-induced lung injury activities in the daily consumption of natural products. In addition, our study also inspires the discovery of new beneficial effects of bixin and its application in the treatment of other inflammatory diseases.

Received 12th November 2017.  
Accepted 10th January 2018

DOI: 10.1039/c7tx00304h

rsc.li/toxicology-research

## Introduction

Particle-induced lung injury is a comprehensive pulmonary disease with progressive inflammation and fibrosis, and SiO<sub>2</sub> exposure caused lung injury is the major one, which ultimately leads to diffuse pulmonary fibrosis, lung structure distortion, and respiratory failure.<sup>1,2</sup> The early stages may be asymptomatic, but the advanced stages of the disease can result in airflow limitation, hypoxia, pulmonary hypertension, respiratory or heart failure, and premature death.<sup>3</sup> During its development, the pulmonary injury develops progressively, even without further exposure to silica particles. Unfortunately,

there are currently no curative treatments for this injury, which makes lung transplantation the only remaining therapy.<sup>4</sup> However, the high cost, limited donor supply, and surgical invasiveness of lung transplantation continue to be challenges. Therefore, the development of an effective alternative treatment is urgently needed.

SiO<sub>2</sub>-induced lung injury is characterized by the deposition of inhaled silica particles, prolonged cycles of massive inflammation, epithelial hyperplasia and the formation of dense nodules with a central hyalinized whorled collagen in the lungs.<sup>5,6</sup> Previous studies have shown that alveolar macrophage activation plays a vital role in the initiation and progression of this injury.<sup>7,8</sup> Activated alveolar macrophages secrete a series of pre-inflammatory cytokines, including IL6, IL8 and TNF $\alpha$ , through the p38/MAPK signaling pathway and NF- $\kappa$ B nuclear translocation, which stimulate the neighboring fibroblasts and macrophages.<sup>9</sup> This process causes fibroblast proliferation and eventually leads to pulmonary fibrosis.<sup>10,11</sup> In addition, phagocytosing silica particles by lung macrophages leads to the generation of reactive oxygen species (ROS) which further exacerbates this lung injury. Endogenous anti-inflammatory and anti-oxidative reactions can also be activated in response to the inflammation and redox imbalance triggered by particle exposure.

<sup>a</sup>Jiangsu Key Laboratory of Preventive and Translational Medicine for Geriatric Disease, School of Public Health, Soochow University, Suzhou, 215123, PR China.

E-mail: taoqishu619@126.com; Fax: +86-0512-65698540; Tel: +86-0512-65698540

<sup>b</sup>School of Public Health, Medical College of Soochow University, 199 Ren'ai Road, Suzhou 215123, Jiangsu, China. E-mail: zhangzengli@suda.edu.cn;

Fax: +86-0512-656883323; Tel: +86-0512-656883323

<sup>c</sup>Experimental Center of Medical College, Soochow University, 199 Ren'ai Road, Suzhou 215123, Jiangsu, China

† Electronic supplementary information (ESI) available: S1 – The relative changes of body weight (A) and the relative changes of lung weight of the mice with the indicated treatments (B). See DOI: 10.1039/c7tx00304h

‡ Lian Xue and Hong Zhang equally contributed to this work.

The cellular protective response against oxidative stress is mainly orchestrated by the transcription factor NRF2 (nuclear factor-E2-related factor 2). It regulates the expression of numerous antioxidant, anti-inflammatory, and pro-survival genes with antioxidant response elements (ARE) in their promoters.<sup>12,13</sup> In general, NRF2 is ubiquitously expressed at low levels. However, its expression can be quickly up-regulated in response to various cellular stresses, including stress caused by exogenous particle exposure.<sup>14</sup> In addition, the pre-activation of the NRF2/ARE signaling pathway facilitates an adaptive response that protects against various types of stresses encountered subsequently. Employing natural compounds to activate the NRF2 signaling pathway has been proved to be an effective chemo-preventive strategy, as demonstrated in various preclinical studies.<sup>15–18</sup> In fact, many natural compounds used in traditional medicines for their antioxidant and anti-inflammatory properties have been shown to be NRF2 inducers that elicit a therapeutic effect through the NRF2/ARE signaling pathway.<sup>15–17</sup> Collectively, NRF2 plays a key role in cellular defense against pathological oxidative stress and inflammation.<sup>19,20</sup> It has been previously reported that NRF2 activation in response to chemo-preventive agents or oxidative stress is regulated by KEAP1, a substrate adaptor protein of an E3-ubiquitin ligase which binds to and negatively regulates NRF2.<sup>21,22</sup> Specifically, the critical cysteine residues in KEAP1 can be oxidized by ROS or modified by electrophilic compounds, which releases it from NRF2 and prevents NRF2 from degradation.<sup>23,24</sup>

Bixin is a carotenoid extracted from *Bixa orellana* seeds and is used as a colorant for food, cosmetics and textiles approved by the FDA.<sup>25</sup> Traditionally, in Mexico and South America, bixin was used in the treatment of infections and inflammatory diseases of the skin, prostate, and gastrointestinal tract, as well as chest pain.<sup>26</sup> Our laboratory has previously demonstrated that bixin is able to quench the ROS generated during ventilation-induced acute oxidative lung injury.<sup>25</sup> As a result of its antioxidant properties, bixin successfully prevented oxidative DNA damage and lipid peroxidation.<sup>25,27</sup> Additionally, bixin also attenuated cisplatin-induced clastogenicity and carbon tetrachloride mediated hepatotoxicity.<sup>28</sup> Bixin has been proved to be safe in daily consumption and there is no epidemiological evidence showing carcinogenicity or acute toxicity associated with the ingestion of or the occupational exposure to bixin, except for rare reports of allergies caused by bixin ingestion.<sup>29,30</sup>

To date, multiple natural products have been used for the treatment of SiO<sub>2</sub>-induced lung injury, but their mechanisms are still unclear.<sup>31,32</sup> Applications of monomeric compounds derived from natural products to particle-induced pulmonary disease treatment are rarely reported. The potential protection effects of bixin on the development of this damage have not yet been studied. In this study, we established a murine model with particle exposure through silica intratracheal instillation. We showed that bixin significantly alleviates silica-induced pulmonary inflammation and fibrosis in mice. We also proved that bixin exhibits its cytoprotective effects *via* activating the NRF2 signaling pathway in both *in vivo* and *in vitro* studies.

This study discovered the antioxidant mechanisms of bixin in the treatment of particle-induced lung injury. Our work has brought insights into exploring anti-particle-related pulmonary disease activities among other natural products to contribute to particle-related pulmonary disease medical therapies. Furthermore, our study also inspires the discovery of new beneficial effects of bixin and its application in the treatment of other indications.

## Materials and methods

### Chemicals, antibodies and cell culture

Bixin was purchased from Spectrum (New Brunswick, NJ), tBHQ and silica (SiO<sub>2</sub>) were purchased from Sigma (St Louis, MO), and sulforaphane (SF) was purchased from Santa Cruz (Santa Cruz, CA). MG132 was purchased from Amquar (AMQUAR Bio., Colorado, USA). Primary antibodies against NRF2, KEAP1, GCLM, AKR1C1, P65, p-P65, LC3, and GAPDH were purchased from Santa Cruz. Hemagglutinin (HA) epitope antibody was purchased from Covance (Branford, CT). Ubiquitin antibody was purchased from Sigma. 8-Oxo-dG antibody was purchased from Trevigen (Gaithersburg, MD). Horseradish peroxidase (HRP)-conjugated secondary antibodies were purchased from Immunoway (Plano, TX). Human THP-1 acute monocytic leukemia cells were purchased from ATCC (Manassas, VA). THP-1 cells were cultured in RPMI 1640 medium supplemented with 10% FBS (Hyclone, Logan, UT), 0.1% gentamycin (Invitrogen, Carlsbad, CA) and 5 ng ml<sup>-1</sup> phorbol-12-myristate-13-acetate (PMA) (Sigma). The cells were maintained at 37 °C in a humidified incubator containing 5% CO<sub>2</sub>.

### siRNA silencing and cDNA transfection

The transfection of cDNA was performed using lipofectamine 2000 (Invitrogen). Hiperfect was used for small interfering RNA (siRNA) silencing. *Control siRNA* #1027281 and *NRF2 siRNA* #SI03187289 were purchased from Qiagen. The transfections of cDNA and siRNA were performed according to the manufacturer's instructions.

### Cell viability assay

The potential cytotoxicity of bixin and its cyto-protective effects in THP-1 cells were measured by the functional impairment of the mitochondria using 3-(4,5-dimethylthiazol-2-yl)-2,5-diphenyltetrazolium bromide (MTT) (Sigma). Briefly, approximately 2 × 10<sup>4</sup> THP-1 cells per well were seeded in a 96-well plate followed by 24 h of incubation. The cells were then treated with multiple doses of bixin for 48 h and were subjected to cell viability assay. On the other hand, THP-1 cells were transfected with either *control-siRNA* (*Ctrl siRNA*) or *NRF2-siRNA* (*NRF2 siRNA*) for 24 h. Approximately 2 × 10<sup>4</sup> transfected cells per well were seeded in a 96-well plate and pretreated with DMSO or bixin (40 μM) for 4 h. Cells were then exposed to multiple concentrations of SiO<sub>2</sub> (0–2000 μg ml<sup>-1</sup>) for 48 h. For cell viability measurement, 20 μL of 2 mg mL<sup>-1</sup> MTT was

directly added to the cells followed by incubation at 37 °C for 2 h. 100 µl of isopropanol/HCl was added into each well after MTT incubation. The plate was then put on a shaker at room temperature for 15 min. The absorbance at 570 nm was measured using a Synergy 2 multi-mode microplate reader (Biotek, Seattle, USA). All samples were run in triplicates for each experiment and the data represent the means of three independent experiments.

### ROS detection

THP-1 cells were transfected with either *control-siRNA* (*Ctrl siRNA*) or *NRF2-siRNA* (*NRF2 siRNA*) for 24 h. Approximately  $1.5 \times 10^6$  transfected cells per well were seeded in a 6-well plate. The cells were pretreated with DMSO or bixin (40 µM) for 4 h prior to SiO<sub>2</sub> exposure (0–100 µg ml<sup>-1</sup>) for 24 h. The cells were then washed with PBS followed by incubation with fresh medium containing 2',7'-dichlorodihydrofluorescein diacetate (H<sub>2</sub>DCFDA) (Sigma, St Louis, MO, 10 µg ml<sup>-1</sup> final concentration) for 30 min at 37 °C. The cells were then rinsed with PBS twice and trypsinized and resuspended in PBS to approximately  $10^6$  cells per ml. Fluorescence was measured using flow cytometry with excitation at 488 nm and emission at 515–545 nm. The procedures following H<sub>2</sub>DCFDA incubation were performed in the dark.

### Immunoblot analysis, ubiquitination assay and protein half-life

THP-1 cells were harvested in Laemmli buffer (62.5 mM Tris-HCl (pH 6.9), 3% SDS, 10% glycerol, 5% beta-mercaptoethanol, and 0.1% bromophenol blue). Cell lysates were sonicated on ice to allow full digestion followed by boiling for 10 min. The denatured lysates were electrophoresed through an SDS-polyacrylamide gel and subjected to immunoblot analysis. For endogenous ubiquitination assay, THP-1 cells were left untreated (control) or treated with bixin (40 µM) along with MG132 (10 µM) for 4 h. For exogenous ubiquitination assay, THP-1 cells were first co-transfected with the expression vectors of HA-tagged ubiquitin and NRF2 for 24 h. The cells were then left untreated or treated with SF (5 µM), tBHQ (40 µM) or bixin (40 µM) along with MG132 (10 µM) for 4 h. At the completion of the treatments, the cells were harvested in a digesting buffer containing 2% SDS, 150 mM NaCl, 10 mM Tris-HCl (pH 8.0), and 1 mM DTT and were immediately boiled. For immunoprecipitation, cell lysates were incubated with 1 µg of NRF2 antibody along with protein A agarose beads (Invitrogen) at 4 °C overnight. The immunoprecipitated complexes were then washed with a buffer containing 0.5 M LiCl/TBS and 1 mM DTT followed by two additional washes with a buffer containing 1% Triton-X-100/TBS and 1 mM DTT. The immunoprecipitated protein was then eluted in Laemmli buffer followed by boiling for 10 min. The samples were resolved by SDS-PAGE and analyzed by immunoblotting with the antibodies against ubiquitin (endogenous ubiquitination assay) and the HA epitope (exogenous ubiquitination assay). To measure the half-life of NRF2, THP-1 cells were either left untreated or treated with 40 µM bixin for 4 hours. 50 µM cyclo-

heximide was then added to block protein synthesis. Total cell lysates were collected at different time points and were subjected to immunoblot analysis with an anti-NRF2 antibody. The relative intensities of the immunoblot bands were quantified using the Syngene gel documentation system and GeneTools software from Syngene (Frederick, MD).

### mRNA extraction and real-time RT-PCR

Total RNA was extracted from THP-1 cells and mice lung tissues using TRIzol reagent from CWBIO (Beijing, China). Equal amounts of mRNA were used to generate cDNA using a HiFiScript cDNA synthesis kit following the manufacturer's instructions (CWBIO, Beijing, China). The RT-PCR procedures and primer sequences of *NRF2*, *KEAP1*, *GCLM*, *AKR1C1* and *GAPDH* were described previously.<sup>25,27,33</sup> ABI 7500 (Applied Biosystems) was used to evaluate mRNA expression. The quantification of the cDNA expression of mouse *Nrf2*, *Keap1*, *Gclm*, *Akr1c1*, *Il6* and *Trfa* in the lung tissue samples was performed using an UltraSYBR Mixture (Low ROX) qPCR kit (CWBIO, Beijing, China). The primers were designed with Primer 3 ([http://www-genome.wi.mit.edu/genome\\_software/other/primer3.html](http://www-genome.wi.mit.edu/genome_software/other/primer3.html)) and were synthesized by Genewiz. The sequences of the primers are listed as follows:

*Nrf2*: forward (CTCAGCATGATGGACTTGGGA);  
reverse (TCTTGCCTCCAAAGGATGTC);  
*Keap1*: forward (GATCGGCTGCACTGAACTG);  
reverse (GGCAGTGTGACAGGTTGAAG);  
*Akr1c1*: forward (GGAGGCCATGGAGAAGTGTA);  
reverse (GCACACAGGCTTGTACCTGA);  
*Gclm*: forward (TCCCATGCAGTGGAGAAGAT);  
reverse (AGCTGTGCAACTCCAAGGAC);  
*β-actin*: forward (AAGGCCAACCGTGAAAAGAT);  
reverse (GTGGTACGACCAGAGGCATAC).

The real-time PCR conditions used were: initial denaturation (95 °C, 10 min), 40 cycles of amplification (95 °C, 10 s; 60 °C, 30 s; 72 °C, 32 s), melting curve (95 °C, 15 s; 60 °C, 1 min; 95 °C, 15 s), and cooling cycle (60 °C, 15 s). The mean crossing point (Cp) values and standard deviations (SD) were determined. The Cp values were normalized to the respective Cp values of the mouse *β-actin* reference gene. The data are presented as a fold change in gene expression compared to the control group.

### Animals and treatments

Male C57BL/6 mice (7 weeks old) were purchased from SLAC Laboratory Animal Co. Ltd (Shanghai, China) and were maintained in 12 h light/dark cycle, climate-controlled and pathogen-free rooms. All mice were fed with standard mouse chow, and permitted food and water consumption *ad libitum*. Mice handling in this study followed the Guide for the Care and Use of Laboratory Animals and the study protocols were approved by the Soochow University Institutional Animal Care and Use Committee (permission number: SYXK 2014-0030). Eight-week-old mice were randomly allocated into four experimental groups ( $n = 18$  per group): (i) control (tea oil); (ii) bixin (200 mg kg<sup>-1</sup>, dissolved in tea oil); (iii) SiO<sub>2</sub>; and (iv) bixin + SiO<sub>2</sub>.

The mice were first intratracheally instilled with SiO<sub>2</sub> (3 mg in 50 µl sterile saline). Bixin was administered by intraperitoneal (i.p.) injection every three days (starting from 72 h before SiO<sub>2</sub> intratracheal instillation) until the end of the experiment. The mice were weighed once a week during the experiments before they were euthanized at day 7, day 28, and day 56 following SiO<sub>2</sub> instillation ( $n = 6$  per group).

### Silica preparation

The content of the free SiO<sub>2</sub> dust was more than 99%, and the particle size of 80% of the SiO<sub>2</sub> dust was between 1 and 5 µm. Silica was ground in saline for 3 h, and boiled in 1 N HCl. After washing, the particles were resuspended in sterile saline. The suspensions were subjected to sonication for 10 min before use.

### Bronchoalveolar lavage (BAL) and lung tissue collection

After the completion of the treatments, the mice were euthanized and BAL fluids were obtained by lavaging the lungs with 1 mL HBSS (Invitrogen) through a tracheal cannula.<sup>34</sup> The BAL fluid was centrifuged at 500g for 20 min at 4 °C to collect the cells. The cell pellets were then resuspended in PBS and the total cell counts were determined using a TC20 automated cell counter (BioRad). The rest of the BAL cells were subjected to cytopspin (Cytospin 4, Thermo Fisher Scientific) preparation as previously reported and slides were stained with a Shandon Kwik-Diff kit (Thermo Fisher Scientific).<sup>25</sup> Macrophages, neutrophils and lymphocytes were identified based on standard morphological criteria and in total 200 cells were examined per sample. The mean cell counts ± SD were obtained from 6 mice from each group. The BAL fluid supernatants were centrifuged again at 15 000g for 10 min at 4 °C and were stored at −80 °C for protein analysis. Lung tissues from each experimental group were harvested and divided into two parts: one part was frozen in liquid nitrogen for total RNA extraction and protein analysis and the other part was fixed in 10% buffered formalin and embedded in paraffin for histological and immunochemical analysis.

### H&E (hematoxylin and eosin) and IHC (immunohistochemical) staining

Lung tissue sections (4 µm) were baked and deparaffinized. H&E staining was performed for pathology analysis. IHC analysis was performed as previously described.<sup>18</sup> Briefly, antigen retrieval was performed by boiling the slides with a retrieval solution (citric acid monohydrate 2.1 g L<sup>−1</sup> in H<sub>2</sub>O, pH = 6.0) three times (5 min each time). The tissue sections were then exposed to 3.5 M HCl for 15 min at room temperature and washed with PBS three times for 5 min each time. Subsequently, the tissue sections were treated with 0.3% peroxidase to quench endogenous peroxidase activity. The tissue sections were blocked for 30 min with 5% normal goat serum followed by 2 h of incubation with NRF2 antibody at 1:100 dilution at room temperature. Staining was performed using an EnVision+System-HRP kit (Dako) following the manufacturer's instructions.

### IHC analysis for 8-hydroxy-2'-deoxyguanosine (8-oxo-dG)

Tissue sections were baked and deparaffinized. IHC analysis for 8-oxo-dG was performed as previously described.<sup>25</sup> Briefly, lung tissue sections were incubated with proteinase K (800 U ml<sup>−1</sup>, in PBS) for 20 min at 37 °C, followed by washing with PBS 3 times (5 min each time). The sections were then treated with RNase A (10 mg ml<sup>−1</sup> in a buffer containing 150 mM NaCl and 15 mM sodium citrate) for 1 h at 37 °C and washed with PBS 3 times (5 min each time). After the DNA in the tissue sections was denatured with 2 N HCl for 5 min at room temperature, the sections were neutralized with 1 M Tris-base for 5 min. Subsequently, the sections were blocked with 5% normal goat serum for 30 min followed by 2 h of incubation with 8-oxo-dG antibody at 1:5000 dilution at room temperature. Staining was performed using an EnVision+System-HRP kit (Dako) according to the manufacturer's instructions.

### In situ TUNEL assay

Apoptotic cell death in lung tissues was measured using an *in situ* cell death detection kit (Roche) following the manufacturer's instructions. Briefly, the tissue sections were pretreated with proteinase K (800 U ml<sup>−1</sup>) in 10 mM Tris/HCl (pH = 7.8) at 37 °C for 30 min. The sections were then washed 3 times with PBS followed by incubation with a TUNEL reaction mixture for 1 h at 37 °C in the dark. The tissue sections were then stained with Hoechst stain, and were analyzed using a fluorescence microscope (LEICA DM 2500; excitation wavelength: 450–500 nm; detection wavelength: 515–565 nm; Hoechst stain was visualized under UV light).

### Statistics

The results are presented as fold changes to the control groups. The data are shown as mean ± SD of three independent experiments performed in duplicate (real-time RT-PCR) or triplicate (MTT and ROS detection). Statistical tests were performed using SPSS 20.0. Unpaired Student's *t*-test was applied to compare the means of two groups. One-way ANOVA with *Bonferroni's* correction was applied to compare the means of three or more groups. A value of  $p < 0.05$  was considered to be significant.

## Results

### Bixin protects against SiO<sub>2</sub>-induced lung tissue damage

To investigate the potential protective effects of bixin on the development of lung injury caused by SiO<sub>2</sub> exposure, mice were instilled with SiO<sub>2</sub> (3 mg in 50 µl sterile saline) intratracheally on day 0. Bixin (200 mg kg<sup>−1</sup>) or control vehicle (tea oil) were given three days before SiO<sub>2</sub> instillation and every three days after the exposure until they were euthanized on day 7, day 28 and day 56 (Fig. 1A). There were no significant differences in the body weight and lung weight among each experimental group (S1†). First, to evaluate the general lung tracheal epithelium injuries induced by SiO<sub>2</sub>, the total BAL protein amount from each experimental group of mice at indicated

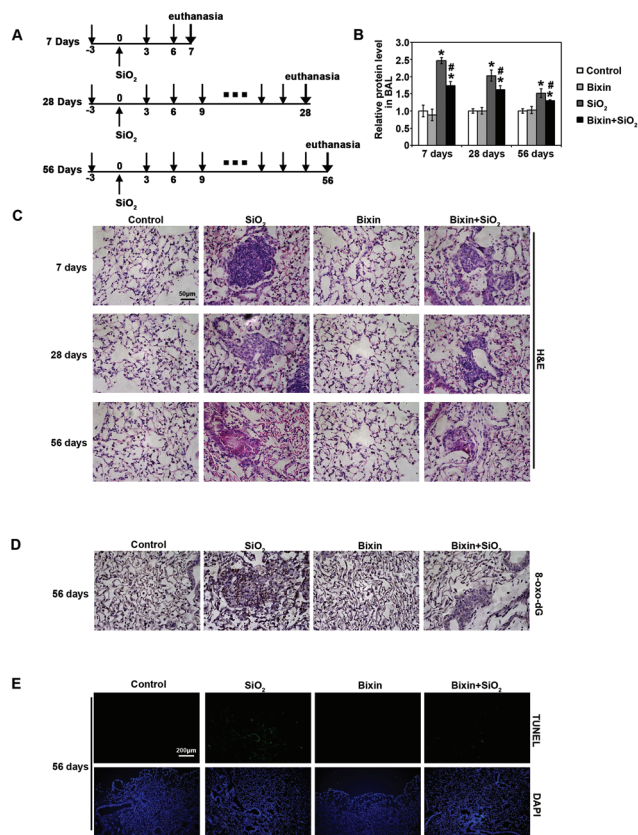


**Fig. 1** Bixin protects against SiO<sub>2</sub>-induced tissue damage. (A) Three different time points of the experiments performed: 7 days, 28 days and 56 days. Treatment regimens: the respective groups of mice received i.p. injection of carrier control (tea oil) or bixin (200 mg kg<sup>-1</sup>) three days before the SiO<sub>2</sub> exposure and every three days after. SiO<sub>2</sub> was intratracheally instilled at day 0. The mice were harvested at 7 days, 28 days and 56 days. (B) Total BAL protein amount from the indicated treatment groups at different time points was measured. The data are presented as mean  $\pm$  SD (\**p* < 0.05, control vs. treatment groups; #*p* < 0.05, SiO<sub>2</sub> vs. bixin + SiO<sub>2</sub>). (C) H&E staining of lung tissue sections from the respective groups of mice at different time points was performed. (D) IHC of 8-oxo-dG and (E) *in situ* TUNEL analysis (visualizing apoptotic cells) of lung tissue sections after SiO<sub>2</sub> intratracheal instillation for 56 days were performed [*n* = 6, the representative images of the lung tissue from each group are shown (scale bar: 50  $\mu$ m)].

time points was measured (Fig. 1B). The total protein level in the BAL fluid increased by  $\sim$ 2.5-fold as compared to the control group after 7 days of SiO<sub>2</sub> exposure. With longer exposure durations, the protein levels decreased, but they remained significantly higher than that in the control group. In addition, the elevated BAL protein levels induced by SiO<sub>2</sub> exposure were substantially reduced with bixin co-treatment at all time points. Bixin alone had no effects on the basal BAL protein levels. These data suggest protective effects of bixin on SiO<sub>2</sub> instillation mediated alveolar leakage.

Next, to investigate the effects of SiO<sub>2</sub>-induced lung injury and the protective effects of bixin during the disease development, the lung tissues collected at each time point were subjected to pathology analysis (Fig. 1C). H&E staining of the lung

tissues revealed that SiO<sub>2</sub> exposure caused the infiltration of inflammatory cells and alveolar septal thickening starting at day 7 post-instillation, as compared to the control group. In addition, irregular cellular nodules were observed at day 7 with SiO<sub>2</sub> exposure. Bixin injection alone did not affect the lung morphology; however, it dramatically attenuated the pulmonary pathological changes caused by SiO<sub>2</sub> instillation. This inflammatory response decreased at day 28 post-instillation, and clear fibrosis began to form across the cellular nodules, which indicated that the cellular nodules were transformed into cellular fibrotic nodules. In addition, the size of the cellular nodules also decreased. At day 56, the inflammation of the lungs with SiO<sub>2</sub> exposure was evidently resolved, and the majority of the cellular fibrotic nodules became mostly fibrotic (fibrotic cellular nodules). In contrast, bixin treatment dramatically decreased the size of nodules starting at day 7. In addition, the fibrotic cellular nodules were dramatically shrunk, and the fibrotic level of the nodules was also significantly decreased at day 56 post-exposure. Collectively, these results indicated that SiO<sub>2</sub> instillation caused a pronounced lung inflammation, which progressed from initial irregular cellular nodules to fibrotic nodules. However, bixin significantly attenuated the pulmonary inflammation and the subsequent lung fibrosis caused by SiO<sub>2</sub> exposure.

SiO<sub>2</sub> mediated oxidative DNA damage during the development of lung injury was also determined by 8-oxo-dG staining. As shown in Fig. 1D, SiO<sub>2</sub> instillation markedly enhanced oxidative DNA damage in the lung tissue after 56 days of exposure, which was significantly suppressed with bixin cotreatment. Bixin treatment alone did not have any effects, indicating that there was no pro-oxidant effects at the dose of bixin used (Fig. 1D). Consistent with this observation, TUNEL analysis also showed that the apoptotic cell death caused by SiO<sub>2</sub> exposure was dramatically reduced by bixin cotreatment (Fig. 1E). In summary, these observations suggest that bixin exhibits protective effects on SiO<sub>2</sub>-mediated pulmonary injury *via* reducing inflammation, oxidative DNA damage and cell apoptosis.

### Bixin attenuates SiO<sub>2</sub>-induced injury by decreasing P65 phosphorylation in the lung tissues

In addition to the pathological changes, silica particle inhalation also induces lung inflammation, which is characterized by the accumulation of inflammatory cells and secretion of pro-inflammatory cytokines. We first quantified the total and distinct inflammatory cell types in BAL to further our understanding of the pathological observations. SiO<sub>2</sub> instillation induced dramatic inflammatory cell infiltration as assessed by the increase in the total cell numbers as well as the numbers of macrophages, neutrophils, or lymphocytes on day 7, 28, and 56 (Fig. 2A–D). Bixin treatment alone did not have any effect on cell infiltration; however, it significantly reduced inflammatory cell infiltration (total, macrophages, neutrophils, and lymphocytes) mediated by SiO<sub>2</sub> exposure at all of the time points. We then measured the mRNA levels of the pro-inflammatory cytokines (*Il6* and *Tnfa*) which are surrogate markers for the

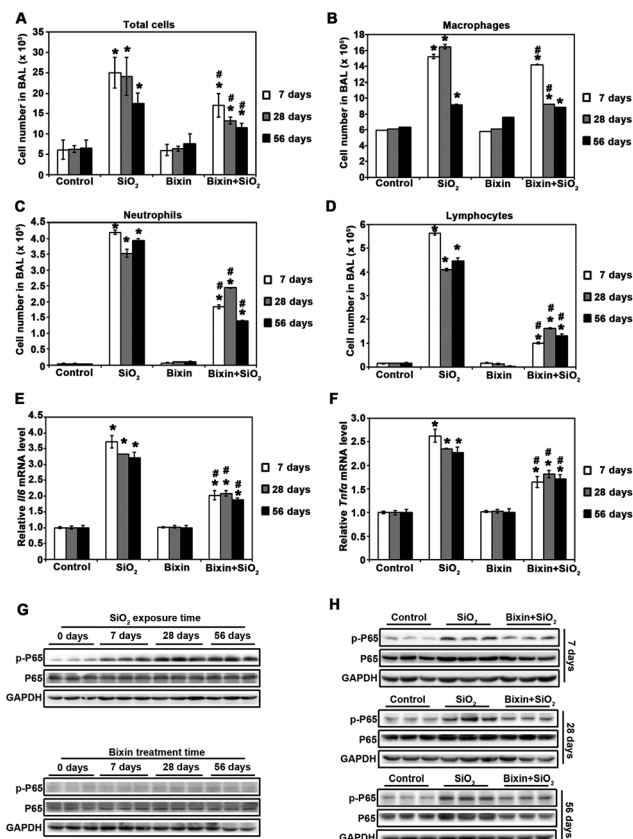


**Fig. 2** Bixin attenuates SiO<sub>2</sub>-induced inflammation by decreasing P65 phosphorylation in the lung tissues. (A) Total cell numbers in BAL were measured in the indicated treatment groups. Cell differential analysis was performed on the BAL cells for each mouse sample. Cell numbers of (B) macrophages, (C) neutrophils and (D) lymphocytes were counted ( $n = 6$ ). The mRNA levels of (E) *Il6* and (F) *Tnfa* were measured by RT-PCR analysis. The results are expressed as mean  $\pm$  SD (\* $p < 0.05$ , control vs. treatment groups; # $p < 0.05$ , SiO<sub>2</sub> vs. bixin + SiO<sub>2</sub>). Lung tissue lysates from the indicated groups of mice ( $n = 3$ ) were subjected to immunoblot analysis with the NF- $\kappa$ B signaling pathway (P65, p-P65) antibodies.

activation of the NF- $\kappa$ B signaling pathway using real-time RT-PCR. SiO<sub>2</sub> exposure greatly induced the mRNA expressions of *Il6* and *Tnfa*, which were both blocked by bixin treatment at all of the time points (Fig. 2E and F). We then investigated the activation of the NF- $\kappa$ B signaling pathway through measuring the phosphorylation of its P65 subunit. SiO<sub>2</sub> exposure dramatically induced the phosphorylated (active) form of P65 (p-P65), while the total P65 protein level remained unchanged (Fig. 2G). In contrast, bixin treatment successfully blocked the phosphorylation of p-P65 mediated by SiO<sub>2</sub> without reducing the total protein level (Fig. 2H). Collectively, our data suggest that bixin reduces SiO<sub>2</sub> mediated pulmonary inflammation through blocking P65 phosphorylation in the lung tissues.

### Bixin induces the NRF2 signaling pathway in the lung tissues

To explore the mechanism of bixin's protective effects on SiO<sub>2</sub>-induced lung injury, the activities of the NRF2 signaling

pathway were determined in each experimental group. Consistent with our previous discovery of bixin's antioxidant activities,<sup>25</sup> we here showed that bixin treatment markedly increased the protein expression of NRF2 and its target GCLM, as assessed by IHC staining of the lung tissues. Particle exposure has been previously reported to induce the NRF2 signaling pathway, and as expected, elevated NRF2 expression was observed with SiO<sub>2</sub> exposure.<sup>18,35</sup> In addition, an increased NRF2 expression was also detected in the combination exposure to bixin and SiO<sub>2</sub> (Fig. 3A). This observation was confirmed by immunoblot analyses of the total protein extracted from the lung tissue collected at all time points, where we showed that the protein expression of NRF2 and its targets (GCLM and AKR1C1) was induced by bixin and SiO<sub>2</sub> exposure (either alone or in combination), and there is no effect on

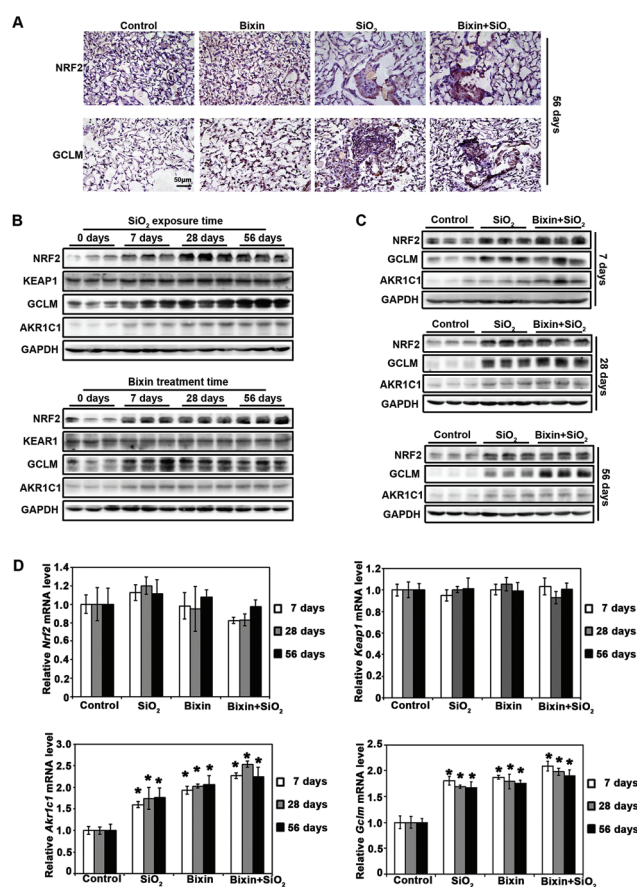


**Fig. 3** Bixin induces the NRF2 signaling pathway in the lung tissues. (A) IHC staining of NRF2 and its target GCLM in the lung tissue sections from the indicated treatment groups after 56 days of SiO<sub>2</sub> exposure was performed [ $n = 6$ , a representative image of the lung tissue for each group is shown (scale bar: 50  $\mu$ m)]. (B) Lung tissue lysates from SiO<sub>2</sub> and bixin groups were subjected to immunoblot detection of the NRF2 pathway antibodies at the indicated time points. (C) Lung tissue lysates from the control, SiO<sub>2</sub> and bixin + SiO<sub>2</sub> treatment groups were subjected to immunoblot analyses with the NRF2 pathway antibodies at the indicated time points. (D) The mRNA levels of *Nrf2*, *Keap1*, *Akr1c1*, and *Gclm* were measured by RT-PCR analysis. The results are expressed as mean  $\pm$  SD (\* $p < 0.05$ , control vs. treatment groups).

KEAP1 expression (Fig. 3B and C). Furthermore, the mRNA levels of *Nrf2*, *Keap1*, *Akr1c1*, and *Gclm* were also assessed (Fig. 3D). The *Nrf2* mRNA level was not affected by the treatments with bixin or SiO<sub>2</sub>, which is consistent with our previous reports.<sup>25,27</sup> In addition, bixin had no effects on the mRNA levels of *Keap1* as we expected. However, the mRNA expressions of *Akr1c1* and *Gclm* were significantly induced by the exposure to bixin and SiO<sub>2</sub> (either alone or in combination) in the lung tissues. These data suggest that NRF2 is an important regulator in the inflammatory response, and that the protective effects of bixin on SiO<sub>2</sub>-induced lung injury may be conducted through the NRF2 signaling pathway.

### Bixin upregulates the NRF2 signaling pathway in THP-1 cells

The process of SiO<sub>2</sub>-induced lung injury is initiated by macrophage activation in the lung tissues. Previous studies have shown that silica particle exposure can activate lung macrophages, followed by the activation of the NF- $\kappa$ B signaling pathway and induction of the apoptosis associated signaling pathways.<sup>7,36</sup> To gain insights into the mechanism of bixin's protective effects on SiO<sub>2</sub>-mediated lung injury, the differentiated THP-1 cells were utilized for our *in vivo* study. We hypothesize that bixin can block the SiO<sub>2</sub> mediated activation of the NF- $\kappa$ B signaling pathway, which plays critical roles in macrophage infiltration and fibrotic formation in lung injury. Based on the chemical structure of bixin and the previous data in our lab (Fig. 4A), we needed to first determine if bixin has any cytotoxicity before investigating its capability for NRF2 induction in THP-1 cells. The cells were treated with bixin (0–640  $\mu$ M) for 48 h followed by cell viability measurement using the MTT assay. The result showed that cell viabilities were not significantly affected by bixin administration at dosage levels below 160  $\mu$ M (Fig. 4B). We then tested the effects of bixin treatment on regulating the NRF2 signaling pathway. As shown in Fig. 4C and D, bixin treatments markedly up-regulated the protein levels of NRF2 (4 h) as well as its downstream targets (AKR1C1 and GCLM) (16 h) in a dose-dependent manner. Meanwhile, no changes were observed in KEAP1 expression (Fig. 4C). We then picked 40  $\mu$ M and 80  $\mu$ M as treatment dosages in the subsequent time course studies, as bixin at these two dosages can visibly induce NRF2 and its downstream targets without affecting the cell viability. As shown in Fig. 4D and E, the increase in the NRF2 protein levels started as early as 2 h after bixin treatment. This increase peaked during 4 to 8 h post-treatment followed by returning to its basal levels by 24 h (Fig. 4D and E). In addition, an increase in the AKR1C1 and GCLM protein levels occurred at 8 h post-bixin treatment and peaked at 48 h. No change was observed in the KEAP1 protein levels. On the other hand, bixin treatments at 40  $\mu$ M for either 4 or 16 h did not affect the mRNA levels of *NRF2* or *KEAP1* (Fig. 4F and G), as expected of a 'classical' NRF2 inducer.<sup>37</sup> In contrast, bixin significantly increased the mRNA levels of both *AKR1C1* and *GCLM* at 16 h after the treatment, where an increase in the level of *GCLM* occurred as early as 4 h post-treatment (Fig. 4H and I).

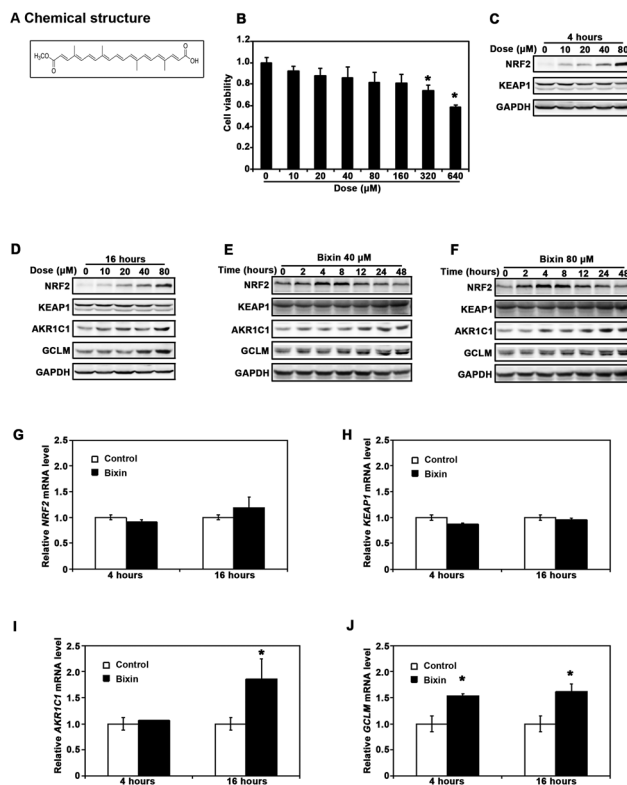


**Fig. 4** Bixin upregulates the NRF2 signaling pathway in THP-1 cells. (A) Bixin chemical structure. (B) Cell viability was measured in THP-1 cells treated with the indicated doses of bixin for 48 h. THP-1 cells were treated with the indicated doses of bixin for (C) 4 h and (D) 16 h. Cell lysates were subjected to immunoblot analyses with the NRF2 signaling pathway antibodies. THP-1 cells were treated with (E) bixin (40  $\mu$ M) and (F) bixin (80  $\mu$ M) for the indicated time points, and the cell lysates were subjected to immunoblot analyses. THP-1 cells were either left untreated (control) or treated with bixin (40  $\mu$ M) for 4 h and 16 h, and mRNA was extracted. The relative mRNA levels of (G) *NRF2*, (H) *KEAP1*, (I) *AKR1C1* and (J) *GCLM* were then determined by quantitative real-time RT-PCR. The data are expressed as mean  $\pm$  SD (\* $p$  < 0.05, control vs. bixin treatment).

### Bixin activates the NRF2 signaling pathway by decreasing NRF2 ubiquitination and increasing NRF2 protein stability

With the evidence showing that bixin is a stronger NRF2 inducer, we then investigated the mechanism of bixin's regulation in the NRF2 signaling pathway. Previous studies have demonstrated that the canonical NRF2 inducers, such as sulforaphane (SF) and Tanshinone-I (T-I), cause NRF2 activation by inhibiting its KEAP1-mediated ubiquitination.<sup>15,17,18</sup> According to bixin's chemical structure, we postulate that bixin activates NRF2 in a similar mechanism. Therefore, cell-based ubiquitination assays were performed. For the exogenous ubiquitination assay, THP-1 cells were co-transfected with the expression vectors of HA-tagged ubiquitin and NRF2. The transfected cells were left untreated or treated with SF (5  $\mu$ M), tBHQ (40  $\mu$ M) or bixin (40  $\mu$ M) along with MG132 (10  $\mu$ M) for 4 h. For the endogenous ubiquitination assay, THP-1 cells were left untreated (control) or treated with bixin (40  $\mu$ M) along

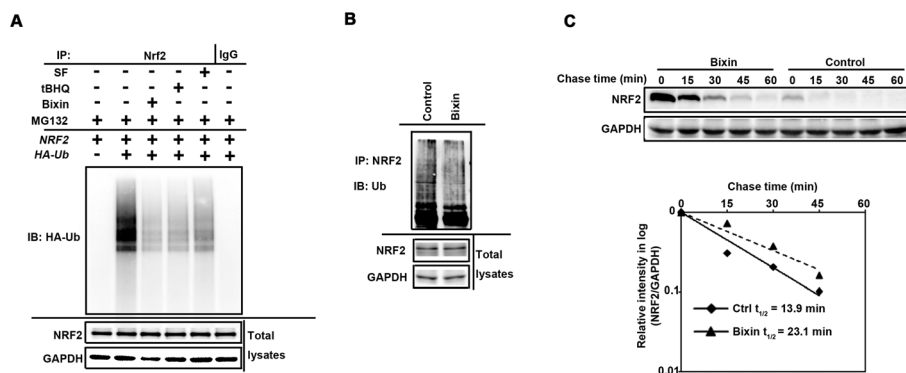


**Fig. 5** Bixin activates the NRF2 signaling pathway by decreasing NRF2 ubiquitination and increasing NRF2 protein stability. (A) THP-1 cells were cotransfected with plasmids encoding the indicated proteins for 24 h. The transfected cells were treated with SF (5  $\mu$ M), tBHQ (40  $\mu$ M) or bixin (40  $\mu$ M) along with MG132 (10  $\mu$ M) for 4 h. Anti-NRF2 immunoprecipitates were analyzed by immunoblotting with anti-HA antibody for the detection of ubiquitin-conjugated NRF2. (B) THP-1 cells were treated with bixin (40  $\mu$ M) along with MG132 (10  $\mu$ M) for 4 h. Anti-NRF2 immunoprecipitates were analyzed by immunoblotting with ubiquitin antibody for the detection of endogenous ubiquitin-conjugated NRF2. (C) THP-1 cells were either left untreated or treated with bixin (40  $\mu$ M) for 4 h. Cycloheximide (CHX, 50  $\mu$ M) was added and the cells were lysed at the indicated time points. Cell lysates were subjected to immunoblot analysis using anti-NRF2 and anti-GAPDH antibodies. The intensities of the bands were quantified using the GeneTools software and plotted against time after CHX treatment to obtain the half-life values.

with MG132 (10  $\mu$ M) for 4 h. Similar to SF and tBHQ, the widely used NRF2 inducers, bixin treatment markedly reduced the ubiquitination level of NRF2 as compared to the untreated control (Fig. 5A and B); to further support the observation that bixin activates the NRF2 signaling pathway by attenuating its ubiquitination, the half-life of the endogenous NRF2 protein was determined. THP-1 cells were either left untreated or treated with 40  $\mu$ M bixin for 4 hours. 50  $\mu$ M cycloheximide was added to block protein synthesis. Total cell lysates were collected at different time points and subjected to immunoblot analysis with an anti-NRF2 antibody (Fig. 5C, upper panel). Quantification of the NRF2 immunoblot bands was performed and the results were plotted and the half-life of NRF2 was calculated (Fig. 5C, lower panel). The half-life of NRF2 of the untreated cells was 13.9 min; however, bixin treatment elongated the NRF2 half-life to 23.1 min. These results indicate that bixin activates NRF2 by blocking its ubiquitination and enhancing NRF2 protein stability.

### Bixin reduces NF- $\kappa$ B mediated inflammation response and prevents SiO<sub>2</sub> caused cell damage in an NRF2-dependent manner

With the knowledge that bixin can activate the NRF2 signaling pathway in THP-1 cells, we then wonder if bixin has cytoprotective effects upon SiO<sub>2</sub> exposure. We first investigated bixin's regulation of the NF- $\kappa$ B signaling pathway induced by SiO<sub>2</sub> exposure. THP-1 cells were pretreated with DMSO (Ctrl) or bixin (40  $\mu$ M) for 4 h followed by exposure to SiO<sub>2</sub> (0–100  $\mu$ g ml<sup>-1</sup>) for an additional 24 h. Consistent with our observations in Fig. 3, both SiO<sub>2</sub> and bixin induced the protein expression of NRF2, GCLM, and AKR1C1. In addition, SiO<sub>2</sub> significantly increased the phosphorylation of P65 without changing the total protein levels of P65. Bixin treatment alone did not have any effect on the protein expression levels of p-P65

and P65. However, the treatment of bixin dramatically reduced the phosphorylation of P65 induced by SiO<sub>2</sub> exposure. Autophagy is a process that can be induced by intracellular stress. SiO<sub>2</sub> mediated cell stress was represented by the increased protein expression of LC3 II, which is a classic autophagy indicator. However, the induced cellular stress was blocked by bixin treatment (Fig. 6A). To confirm this observation and to further explore the mechanism of bixin's protective effects, ROS production and cell viability were measured in THP-1 cells. For the cell viability study, THP-1 cells were transfected with either *control-siRNA* (*Ctrl siRNA*) or *NRF2-siRNA* (*NRF2 siRNA*) for 24 h. The cells were then pretreated with DMSO or bixin (40  $\mu$ M) for 4 h before the addition of the indicated dose of SiO<sub>2</sub> (0–2000  $\mu$ g ml<sup>-1</sup>). Cell viability was measured at 48 h after exposure to SiO<sub>2</sub>. Bixin pretreatment markedly improved cell viability in response to SiO<sub>2</sub> exposure (Fig. 6B). However, this protective effect is gone when the NRF2 protein expression was silenced by *NRF2-siRNA* (Fig. 6C). The ROS activation was blocked by bixin co-treatment. Bixin treatment alone did not affect ROS production, indicating that the dosages of bixin used did not trigger any intracellular oxidative stress (Fig. 6D). However, bixin failed to suppress ROS production in THP-1 cells in the presence of *NRF2-siRNA*, indicating that bixin is able to maintain the cellular redox balance upon SiO<sub>2</sub> challenge and, therefore, protects the cells against SiO<sub>2</sub>-induced cell death.

## Discussion

SiO<sub>2</sub>-induced lung injury is a form of lung disease caused by the inhalation of crystalline silica dust. It is characterized by massive inflammation and scarring in the form of nodular lesions in the upper lobes of the lungs. Despite the work of many previous studies, a cure has not yet been discovered.



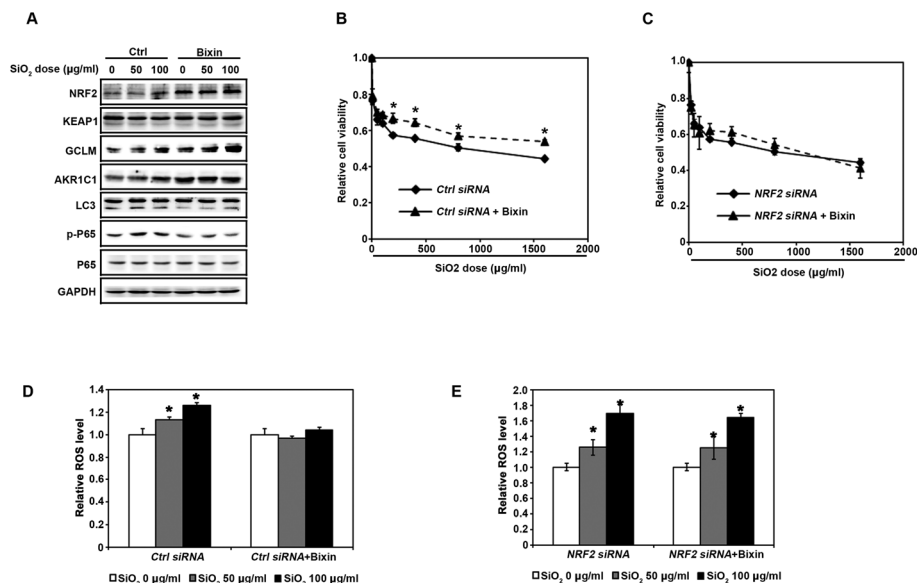


**Fig. 6** Bixin decreases the NF- $\kappa$ B inflammation response and protects against the cell damage induced by the SiO<sub>2</sub> administration in an NRF2-dependent manner. (A) THP-1 cells were pretreated with DMSO (Ctrl) or bixin (40  $\mu$ M) for 4 h prior to the treatment with SiO<sub>2</sub> (0–100  $\mu$ g ml<sup>-1</sup>) for an additional 24 h. Cell lysates were subjected to immunoblot analysis with the indicated antibodies. THP-1 cells were transfected with either (B) *control-siRNA* (Ctrl siRNA) or (C) *NRF2-siRNA* (NRF2 siRNA) for 24 h. The cells were then pretreated with DMSO or bixin (40  $\mu$ M) for 4 h before the addition of the indicated dose of SiO<sub>2</sub> (0–2000  $\mu$ g ml<sup>-1</sup>). Cell viability was measured at 48 h after the addition of SiO<sub>2</sub>. The data are expressed as mean  $\pm$  SD (\* $p$  < 0.05, control vs. bixin treatment). Following the transfection with either (D) *control-siRNA* or (E) *NRF2-siRNA* for 24 h, THP-1 cells were pretreated with DMSO or bixin (40  $\mu$ M) for 4 h prior to the treatment with SiO<sub>2</sub> (0–100  $\mu$ g ml<sup>-1</sup>) for an additional 24 h. DCF-based fluorescence was measured using flow cytometry. The data are expressed as mean  $\pm$  SD (\* $p$  < 0.05, control vs. bixin treatment).

Thus, the treatment of SiO<sub>2</sub>-induced lung injury remains an area of urgent medical need. In addition, the mechanisms of lung inflammation and fibrosis induced by silica particles still need to be explored. In recent years, the applications of natural plant extractions have become promising approaches for the therapeutic treatment of many inflammatory disorders. Bixin has been shown to possess anti-inflammatory properties and exert therapeutic effects on various inflammatory diseases. Our previous studies have shown that bixin was able to inhibit inflammatory cell infiltration in ventilation induced acute lung injury and UV exposure mediated skin damage.<sup>25,27</sup> However, the beneficial effects of bixin on silica-induced lung inflammation and fibrosis have been poorly studied.

In this study, we demonstrated that bixin attenuated silica-induced lung inflammation and fibrosis through up-regulating the NRF2 signaling pathway. We first investigated the protective effects of bixin on the development of SiO<sub>2</sub>-induced lung injury in our *in vivo* mice model. We discovered that silica particle exposure induced the expression of NRF2, GCLM and AKR1C1, which is in agreement with the role of the NRF2 signaling pathway as a stress rescuer (Fig. 3). However, silica exposure also elicited severe inflammatory response (as measured by elevated p-P65 protein and total BAL protein levels, increased total BAL cells, neutrophils, and lymphocytes and increased secretion of inflammatory cytokines) and oxidative stress (as measured by DNA oxidative damage) (Fig. 1 and 2). Bixin induced the expression of NRF2 and its downstream targets in the lung tissues (Fig. 3). Meanwhile, bixin

pretreatment also restored the normal lung morphology and alleviated silica exposure induced inflammation and oxidative stress (Fig. 3). We then proved that bixin is a canonical activator of the NRF2-orchestrated cytoprotective response in human THP-1 acute monocytic leukemia cells (Fig. 4 and 5). Bixin prevented KEAP1 mediated NRF2 ubiquitination which resulted in a prolonged half-life of NRF2. In addition, bixin treatment significantly attenuated the elevated NF- $\kappa$ B inflammatory response and ROS production caused by SiO<sub>2</sub> exposure, which also contributed to the improved cell viability. However, bixin failed to reverse these cell damages when the NRF2 expression was silenced by *NRF2 siRNA* (Fig. 6). Collectively, we demonstrated that bixin reduces the SiO<sub>2</sub> mediated NF- $\kappa$ B inflammatory response and cellular oxidative damage in an NRF2-dependent manner.

NRF2 is widely acknowledged as a major antioxidant and anti-inflammatory factor and its beneficial effects on lung inflammation have been previously reported.<sup>17,18,25</sup> However, the role of NRF2 in SiO<sub>2</sub>-induced lung injury has not yet been well studied. Our group and others have identified that silica particle exposure up-regulates the NRF2 response in lung tissues,<sup>14,35,38,39</sup> and that blocking the NRF2 signaling pathway leads to increased inflammation and oxidative injuries in mice. Yang *et al.* have previously reported that NRF2 activation significantly reduced lung inflammation and fibrosis, and therefore improved the lung structure and function in silica particles instilled mice. They have also proved that earthworm extract could induce NRF2, and protected the lung epithelial

cells against SiO<sub>2</sub>-induced oxidative stress, mitochondrial apoptotic response, and epithelial-mesenchymal transition. Our observation in this study is consistent with their conclusion. Furthermore, we studied the mechanism of bixin's protective effects on lung injury caused by silica exposure.

Alveolar macrophage plays an essential role in lung injury caused by particle inhalation. They are the primary cells that phagocytize inhaled particles in the alveoli which initiates the subsequent pro-inflammatory response and tissue injury.<sup>40,41</sup> Zhang *et al.* reported that silica particle exposure in THP-1 macrophages induced both NF-κB and NRF2 signaling pathways. Their data indicated that the NF-κB signaling pathway is required for the activation of NRF2 and the induction of NRF2-regulated genes in response to SiO<sub>2</sub> particles in macrophages.<sup>38</sup> In contrast, our results showed that bixin treatment induced the NRF2 signaling pathway while it inhibited the NF-κB/P65 signaling pathway, which led to reduced lung inflammatory injury in the mice with silica exposure (Fig. 1–3). In addition, the NF-κB/P65 signaling pathway in the SiO<sub>2</sub> challenged THP-1 macrophage cells was also reduced with bixin treatment (Fig. 6).

The molecular crosstalk between the NRF2 and NF-κB response pathways is complicated. NF-κB regulates the gene expression of a broad range of inflammatory factors including pro-inflammatory cytokines, chemokines, and other stress response proteins.<sup>42</sup> Cytokines such as TNFα and IL-1β or other inflammatory mediators such as cyclooxygenase-2 (COX-2) can activate NADPH oxidases causing increased production of H<sub>2</sub>O<sub>2</sub>, and/or electrophiles, which subsequently activate or induce other redox-sensitive proteins and genes.<sup>43–45</sup> For instance, 15-deoxy-Δ<sup>12,14</sup>-prostaglandin J<sub>2</sub> (15d-PGJ<sub>2</sub>), a product of COX-2, is a well-established NRF2 activator.<sup>46</sup> In addition, other NF-κB-regulated proteins including NADPH oxidase 4 and iNOS that produce oxidants may also activate NRF2 through the direct oxidation of KEAP1 cysteine residues.<sup>47,48</sup> On the contrary, it was previously reported that RAC1, a small G-protein of the Pho family, is involved in the activation of both NF-κB and NRF2 signaling pathways. Specifically, RAC1 can block RAC1-dependent NF-κB activation through inducing NRF2/EpRE signaling.<sup>49</sup> NF-κB/P65 can also compete for co-activators that are required for NRF2 binding with the target DNA, and at the same time NF-κB/P65 can activate histone deacetylase 3 to suppress NRF2-DNA binding.<sup>50</sup> Thus, there should be a balance between the NF-κB and NRF2 signaling pathways. Activating the NRF2 signaling pathway using molecular inducers can be a potential therapeutic method to attenuate the NF-κB signaling pathway mediated inflammatory response, and to protect against tissue injuries from toxicant exposure.

Autophagy is an evolutionarily conserved process during cellular development. During the autophagy process, specific intracellular proteins and organelles can be engulfed by autophagosomes for degradation and recycling.<sup>51</sup> Emerging studies have suggested that ROS production plays an essential role in the activation of the autophagy process.<sup>52</sup> It has been previously reported that silica particle exposure induces auto-

phagy in the macrophage cells, which results in cell activation and apoptosis.<sup>53</sup> This agrees with our observation where we found that bixin treatment reduced the elevated LC3 protein expression levels caused by SiO<sub>2</sub> exposure (Fig. 6A). Additionally, bixin treatment also successfully restored cell viability in THP-1 cells upon SiO<sub>2</sub> exposure (Fig. 6B–C). Consistently, our animal studies demonstrated that bixin treatment significantly suppressed cellular DNA damage and apoptotic cell death induced by SiO<sub>2</sub> exposure (Fig. 1D–E). Taken together, these results suggest that bixin reduces SiO<sub>2</sub>-induced pulmonary injury through suppressing inflammation, oxidative DNA damage and cell apoptosis.

In summary, this present study demonstrates that bixin blocks the NF-κB mediated inflammatory response and prevents SiO<sub>2</sub>-induced cell damage in an NRF2-dependent manner. Bixin is currently one of the most commonly consumed food colorants worldwide distinguished by a long record of dietary and ethnopharmacological use.<sup>29,54</sup> In prior studies, bixin has demonstrated antigenotoxic and antioxidant cytoprotective activities. The systemic availability of oral bixin and its demethylated metabolite norbixin has been documented in rodent studies and healthy human subjects.<sup>55–58</sup> More importantly, the acceptable daily intake (ADI) of bixin over a lifetime does not seem to project any appreciable health risk, which makes bixin surpass other carotenoids to be approved as a food additive.<sup>59</sup> We have demonstrated that bixin exhibits remarkable pulmonary protection effects during the development of SiO<sub>2</sub>-induced lung injury. Together with the reported safety data and systemic availability analysis of bixin, we suggest that bixin based diets can be applied as a novel strategy for the treatment of SiO<sub>2</sub>-induced lung injury.

## Funding information

The work was supported by the following grants: Chinese National Nature Science Foundation (Grant ref: 81703205, 81473008, 81673203); Youth Foundation of Jiangsu Province (Grant ref: BK20160333); China Postdoctoral Science Foundation (Grant ref: 2016M600440, 2017T100402); Natural Science Research in Colleges and Universities of Jiangsu Province (Grant ref: 16KJB330008, 16KJB330009); and Postdoctoral Science Foundation of Jiangsu Province (Grant ref: 1601079C).

## Conflicts of interest

There are no conflicts of interest to declare.

## Acknowledgements

We thank Sherly Huang for editing this manuscript.

## References

- 1 K. Steenland and E. Ward, Silica: a lung carcinogen, *CA-Cancer J. Clin.*, 2014, **64**, 63–69.
- 2 M. I. Greenberg, J. Waksman and J. Curtis, Silicosis: a review, *DM, Dis.-Mon.*, 2007, **53**, 394–416.
- 3 A. S. Laney, E. L. Petsonk and M. D. Attfield, Pneumoconiosis among underground bituminous coal miners in the United States: is silicosis becoming more frequent?, *Occup. Environ. Med.*, 2010, **67**, 652–656.
- 4 C. C. Leung, I. T. Yu and W. Chen, Silicosis, *Lancet*, 2012, **379**, 2008–2018.
- 5 T. N. Perkins, M. A. Dentener, F. R. Stassen, G. G. Rohde, B. T. Mossman, E. F. Wouters and N. L. Reynaert, Alteration of canonical and non-canonical WNT-signaling by crystalline silica in human lung epithelial cells, *Toxicol. Appl. Pharmacol.*, 2016, **301**, 61–70.
- 6 V. Castranova and V. Vallyathan, Silicosis and coal workers' pneumoconiosis, *Environ. Health Perspect.*, 2000, **108**(Suppl 4), 675–684.
- 7 S. Q. Yao, L. W. Rojanasakul, Z. Y. Chen, Y. J. Xu, Y. P. Bai, G. Chen, X. Y. Zhang, C. M. Zhang, Y. Q. Yu, F. H. Shen, J. X. Yuan, J. Chen and Q. C. He, Fas/FasL pathway-mediated alveolar macrophage apoptosis involved in human silicosis, *Apoptosis*, 2011, **16**, 1195–1204.
- 8 P. Misson, S. van den Brule, V. Barbarin, D. Lison and F. Huaux, Markers of macrophage differentiation in experimental silicosis, *J. Leukocyte Biol.*, 2004, **76**, 926–932.
- 9 H. B. Peng, R. X. Wang, H. J. Deng, Y. H. Wang, J. D. Tang, F. Y. Cao and J. H. Wang, Protective effects of oleanolic acid on oxidative stress and the expression of cytokines and collagen by the AKT/NFkappaB pathway in silicotic rats, *Mol. Med. Rep.*, 2017, **15**, 3121–3128.
- 10 C. Orfila, J. C. Lepert, S. Gossart, M. F. Frisach, C. Cambon and B. Pipy, Immunocytochemical characterization of lung macrophage surface phenotypes and expression of cytokines in acute experimental silicosis in mice, *Histochem. J.*, 1998, **30**, 857–867.
- 11 C. Mohr, D. Gemsa, C. Graebner, D. R. Hemenway, K. O. Leslie, P. M. Absher and G. S. Davis, Systemic macrophage stimulation in rats with silicosis: enhanced release of tumor necrosis factor-alpha from alveolar and peritoneal macrophages, *Am. J. Respir. Cell Mol. Biol.*, 1991, **5**, 395–402.
- 12 M. C. Jaramillo and D. D. Zhang, The emerging role of the Nrf2-Keap1 signaling pathway in cancer, *Genes Dev.*, 2013, **27**, 2179–2191.
- 13 T. W. Kensler, N. Wakabayashi and S. Biswal, Cell survival responses to environmental stresses via the Keap1-Nrf2-ARE pathway, *Annu. Rev. Pharmacol. Toxicol.*, 2007, **47**, 89–116.
- 14 J. Yang, T. Wang, Y. Li, W. Yao, X. Ji, Q. Wu, L. Han, R. Han, W. Yan, J. Yuan and C. Ni, Earthworm extract attenuates silica-induced pulmonary fibrosis through Nrf2-dependent mechanisms, *Lab. Invest.*, 2016, **96**, 1279–1300.
- 15 S. Tao, R. Justiniano, D. D. Zhang and G. T. Wondrak, The Nrf2-inducers tanshinone I and dihydrotanshinone protect human skin cells and reconstructed human skin against solar simulated UV, *Redox Biol.*, 2013, **1**, 532–541.
- 16 M. Long, S. Tao, M. Rojo de la Vega, T. Jiang, Q. Wen, S. L. Park, D. D. Zhang and G. T. Wondrak, Nrf2-dependent suppression of azoxymethane/dextran sulfate sodium-induced colon carcinogenesis by the cinnamon-derived dietary factor cinnamaldehyde, *Cancer Prev. Res.*, 2015, **8**, 444–454.
- 17 Y. Zheng, S. Tao, F. Lian, B. T. Chau, J. Chen, G. Sun, D. Fang, R. C. Lantz and D. D. Zhang, Sulforaphane prevents pulmonary damage in response to inhaled arsenic by activating the Nrf2-defense response, *Toxicol. Appl. Pharmacol.*, 2012, **265**, 292–299.
- 18 S. Tao, Y. Zheng, A. Lau, M. C. Jaramillo, B. T. Chau, R. C. Lantz, P. K. Wong, G. T. Wondrak and D. D. Zhang, Tanshinone I activates the Nrf2-dependent antioxidant response and protects against As(III)-induced lung inflammation in vitro and in vivo, *Antioxid. Redox Signaling*, 2013, **19**, 1647–1661.
- 19 T. Jiang, F. Tian, H. Zheng, S. A. Whitman, Y. Lin, Z. Zhang, N. Zhang and D. D. Zhang, Nrf2 suppresses lupus nephritis through inhibition of oxidative injury and the NF-kappaB-mediated inflammatory response, *Kidney Int.*, 2014, **85**, 333–343.
- 20 H. Y. Cho, S. P. Reddy, M. Yamamoto and S. R. Kleeberger, The transcription factor NRF2 protects against pulmonary fibrosis, *FASEB J.*, 2004, **18**, 1258–1260.
- 21 A. Kobayashi, M. I. Kang, H. Okawa, M. Ohtsujii, Y. Zenke, T. Chiba, K. Igarashi and M. Yamamoto, Oxidative stress sensor Keap1 functions as an adaptor for Cul3-based E3 ligase to regulate proteasomal degradation of Nrf2, *Mol. Cell. Biol.*, 2004, **24**, 7130–7139.
- 22 D. D. Zhang, S. C. Lo, J. V. Cross, D. J. Templeton and M. Hannink, Keap1 is a redox-regulated substrate adaptor protein for a Cul3-dependent ubiquitin ligase complex, *Mol. Cell. Biol.*, 2004, **24**, 10941–10953.
- 23 D. D. Zhang and M. Hannink, Distinct cysteine residues in Keap1 are required for Keap1-dependent ubiquitination of Nrf2 and for stabilization of Nrf2 by chemopreventive agents and oxidative stress, *Mol. Cell. Biol.*, 2003, **23**, 8137–8151.
- 24 A. T. Dinkova-Kostova, W. D. Holtzclaw, R. N. Cole, K. Itoh, N. Wakabayashi, Y. Katoh, M. Yamamoto and P. Talalay, Direct evidence that sulfhydryl groups of Keap1 are the sensors regulating induction of phase 2 enzymes that protect against carcinogens and oxidants, *Proc. Natl. Acad. Sci. U. S. A.*, 2002, **99**, 11908–11913.
- 25 S. Tao, M. Rojo de la Vega, H. Quijada, G. T. Wondrak, T. Wang, J. G. Garcia and D. D. Zhang, Bixin protects mice against ventilation-induced lung injury in an NRF2-dependent manner, *Sci. Rep.*, 2016, **6**, 18760.
- 26 Z. Xu and X. Q. Kong, Bixin ameliorates high fat diet-induced cardiac injury in mice through inflammation and oxidative stress suppression, *Biomed. Pharmacother.*, 2017, **89**, 991–1004.

- 27 S. Tao, S. L. Park, M. Rojo de la Vega, D. D. Zhang and G. T. Wondrak, Systemic administration of the apocarotenoid bixin protects skin against solar UV-induced damage through activation of NRF2, *Free Radical Biol. Med.*, 2015, **89**, 690–700.
- 28 P. R. Moreira, M. A. Maioli, H. C. Medeiros, M. Guelfi, F. T. Pereira and F. E. Mingatto, Protective effect of bixin on carbon tetrachloride-induced hepatotoxicity in rats, *Biol. Res.*, 2014, **47**, 49.
- 29 S. J. Stohs, Safety and efficacy of Bixa orellana (achiote, annatto) leaf extracts, *Phytother. Res.*, 2014, **28**, 956–960.
- 30 W. Auttachoat, D. R. Germolec, M. J. Smith, K. L. White Jr. and T. L. Guo, Contact sensitizing potential of annatto extract and its two primary color components, cis-bixin and norbixin, in female BALB/c mice, *Food Chem. Toxicol.*, 2011, **49**, 2638–2644.
- 31 H. N. Zhang, H. T. Xin, W. D. Zhang, C. J. Jin, S. Y. Huang and Y. Zhang, The anti-fibrotic effects of Qidan granule in experimental silicosis, *Zhonghua Yufang Yixue Zazhi*, 2007, **41**, 290–294.
- 32 L. Z. He, Z. H. Huang, H. R. Wang, D. Y. Tu and Z. F. Mao, Shenjincao (Palhinhaea cernua) injection for treatment of experimental silicosis of rats, *J. Pharm. Pharmacol.*, 1998, **50**, 351–354.
- 33 S. Tao, S. Wang, S. J. Moghaddam, A. Ooi, E. Chapman, P. K. Wong and D. D. Zhang, Oncogenic KRAS confers chemoresistance by upregulating NRF2, *Cancer Res.*, 2014, **74**, 7430–7441.
- 34 L. Moreno-Vinasco, H. Quijada, S. Sammani, J. Siegler, E. Letsiou, R. Deaton, L. Saadat, R. S. Zaidi, J. Messana, P. H. Gann, R. F. Machado, W. Ma, S. M. Camp, T. Wang and J. G. Garcia, Nicotinamide phosphoribosyltransferase inhibitor is a novel therapeutic candidate in murine models of inflammatory lung injury, *Am. J. Respir. Cell Mol. Biol.*, 2014, **51**, 223–228.
- 35 C. Guo, Y. Xia, P. Niu, L. Jiang, J. Duan, Y. Yu, X. Zhou, Y. Li and Z. Sun, Silica nanoparticles induce oxidative stress, inflammation, and endothelial dysfunction in vitro via activation of the MAPK/Nrf2 pathway and nuclear factor-kappaB signaling, *Int. J. Nanomed.*, 2015, **10**, 1463–1477.
- 36 B. L. Liu, The study of oxidative injury of alveolar macrophage in the development of silicosis, *Zhonghua Yufang Yixue Zazhi*, 1993, **27**, 10–12.
- 37 X. J. Wang, Z. Sun, W. Chen, Y. Li, N. F. Villeneuve and D. D. Zhang, Activation of Nrf2 by arsenite and monomethylarsonous acid is independent of Keap1-C151: enhanced Keap1-Cul3 interaction, *Toxicol. Appl. Pharmacol.*, 2008, **230**, 383–389.
- 38 H. Zhang, L. Zhou, J. Yuen, N. Birkner, V. Leppert, P. A. O'Day and H. J. Forman, Delayed Nrf2-regulated antioxidant gene induction in response to silica nanoparticles, *Free Radical Biol. Med.*, 2017, **108**, 311–319.
- 39 C. Lin, X. Zhao, D. Sun, L. Zhang, W. Fang, T. Zhu, Q. Wang, B. Liu, S. Wei, G. Chen, Z. Xu and X. Gao, Transcriptional activation of follistatin by Nrf2 protects pulmonary epithelial cells against silica nanoparticle-induced oxidative stress, *Sci. Rep.*, 2016, **6**, 21133.
- 40 G. Oberdorster, E. Oberdorster and J. Oberdorster, Nanotoxicology: an emerging discipline evolving from studies of ultrafine particles, *Environ. Health Perspect.*, 2005, **113**, 823–839.
- 41 A. Peters, B. Veronesi, L. Calderon-Garciduenas, P. Gehr, L. C. Chen, M. Geiser, W. Reed, B. Rothen-Rutishauser, S. Schurch and H. Schulz, Translocation and potential neurological effects of fine and ultrafine particles a critical update, *Part. Fibre Toxicol.*, 2006, **3**, 13.
- 42 H. L. Pahl, Activators and target genes of Rel/NF-kappaB transcription factors, *Oncogene*, 1999, **18**, 6853–6866.
- 43 X. Chen, B. T. Andresen, M. Hill, J. Zhang, F. Booth and C. Zhang, Role of Reactive Oxygen Species in Tumor Necrosis Factor-alpha Induced Endothelial Dysfunction, *Curr. Hypertens. Rev.*, 2008, **4**, 245–255.
- 44 M. Sato, T. Miyazaki, T. Nagaya, Y. Murata, N. Ida, K. Maeda and H. Seo, Antioxidants inhibit tumor necrosis factor-alpha mediated stimulation of interleukin-8, monocyte chemoattractant protein-1, and collagenase expression in cultured human synovial cells, *J. Rheumatol.*, 1996, **23**, 432–438.
- 45 A. Rahman, J. Kefer, M. Bando, W. D. Niles and A. B. Malik, E-selectin expression in human endothelial cells by TNF-alpha-induced oxidant generation and NF-kappaB activation, *Am. J. Physiol.*, 1998, **275**, L533–L544.
- 46 K. Itoh, M. Mochizuki, Y. Ishii, T. Ishii, T. Shibata, Y. Kawamoto, V. Kelly, K. Sekizawa, K. Uchida and M. Yamamoto, Transcription factor Nrf2 regulates inflammation by mediating the effect of 15-deoxy-Delta(12,14)-prostaglandin j(2), *Mol. Cell. Biol.*, 2004, **24**, 36–45.
- 47 A. Manea, L. I. Tanase, M. Raicu and M. Simionescu, Transcriptional regulation of NADPH oxidase isoforms, Nox1 and Nox4, by nuclear factor-kappaB in human aortic smooth muscle cells, *Biochem. Biophys. Res. Commun.*, 2010, **396**, 901–907.
- 48 T. Koga, W. Y. Zhang, T. Gotoh, S. Oyadomari, H. Tanihara and M. Mori, Induction of citrulline-nitric oxide (NO) cycle enzymes and NO production in immunostimulated rat RPE-J cells, *Exp. Eye Res.*, 2003, **76**, 15–21.
- 49 A. Cuadrado, Z. Martin-Moldes, J. Ye and I. Lastres-Becker, Transcription factors NRF2 and NF-kappaB are coordinated effectors of the Rho family, GTP-binding protein RAC1 during inflammation, *J. Biol. Chem.*, 2014, **289**, 15244–15258.
- 50 G. H. Liu, J. Qu and X. Shen, NF-kappaB/p65 antagonizes Nrf2-ARE pathway by depriving CBP from Nrf2 and facilitating recruitment of HDAC3 to MafK, *Biochim. Biophys. Acta*, 2008, **1783**, 713–727.
- 51 N. Mizushima, Autophagy: process and function, *Genes Dev.*, 2007, **21**, 2861–2873.
- 52 R. Scherz-Shouval and Z. Elazar, Regulation of autophagy by ROS: physiology and pathology, *Trends Biochem. Sci.*, 2011, **36**, 30–38.

- 53 H. Liu, Y. Cheng, J. Yang, W. Wang, S. Fang, W. Zhang, B. Han, Z. Zhou, H. Yao, J. Chao and H. Liao, BBC3 in macrophages promoted pulmonary fibrosis development through inducing autophagy during silicosis, *Cell Death Dis.*, 2017, **8**, e2657.
- 54 C. Ulbricht, R. C. Windsor, A. Brigham, J. K. Bryan, J. Conquer, D. Costa, N. Giese, J. Guilford, E. R. Higdon, K. Holmes, R. Isaac, S. Jingst, J. Kats, L. Peery, E. Rusie, A. Savinainen, T. Schoen, T. Stock, S. Tanguay-Colucci and W. Weissner, An evidence-based systematic review of annatto (*Bixa orellana* L.) by the Natural Standard Research Collaboration, *J. Diet. Suppl.*, 2012, **9**, 57–77.
- 55 L. W. Levy, E. Regalado, S. Navarrete and R. H. Watkins, Bixin and norbixin in human plasma: determination and study of the absorption of a single dose of Annatto food color, *Analyst*, 1997, **122**, 977–980.
- 56 A. C. Junior, L. M. Asad, E. B. Oliveira, K. Kovary, N. R. Asad and I. Felzenszwalb, Antigenotoxic and anti-mutagenic potential of an annatto pigment (norbixin) against oxidative stress, *GMR, Genet. Mol. Res.*, 2005, **4**, 94–99.
- 57 S. Somacal, C. G. Figueiredo, A. Quatrin, A. R. Ruviano, L. Conte, P. R. Augusti, M. Roehrs, I. T. Denardin, J. Kasten, M. L. da Veiga, M. M. Duarte and T. Emanuelli, The antiatherogenic effect of bixin in hypercholesterolemic rabbits is associated to the improvement of lipid profile and to its antioxidant and anti-inflammatory effects, *Mol. Cell. Biochem.*, 2015, **403**, 243–253.
- 58 M. Roehrs, C. G. Figueiredo, M. M. Zanchi, G. V. Bochi, R. N. Moresco, A. Quatrin, S. Somacal, L. Conte and T. Emanuelli, Bixin and norbixin have opposite effects on glycemia, lipidemia, and oxidative stress in streptozotocin-induced diabetic rats, *Int. J. Endocrinol.*, 2014, **2014**, 839095.
- 59 O. World Health, *Evaluation of certain food additives and contaminants. Eightieth report of the Joint FAO/WHO Expert Committee on Food Additives*, World Health Organization technical report series, 2016, pp. 1–114, back cover.